






Düzce University Journal of Science & Technology

Research Article

Numerical Analysis and Optimization of $\text{CH}_3\text{NH}_3\text{PbI}_{3-x}\text{Cl}_x$ Based Perovskite Solar Cells

 Musa ÇADIRCI ^{a,*},  Veli Yasin OĞUZ ^a,  Serhat ERTAN ^a

^a *Electrical&Electronics Engineering, Faculty of Engineering, Düzce University, Düzce, TURKEY*

* *Corresponding author's e-mail address: musacadirci@duzce.edu.tr*

DOI: 10.29130/dubited.831732

ABSTRACT

Due to unique properties of perovskite materials, the solar cells technologies based on those materials rapidly advance to the maximum theoretical conversion efficiency of about 32 %. This study reports the simulation results of $\text{CH}_3\text{NH}_3\text{PbI}_{3-x}\text{Cl}_x$ based perovskite solar cells using SCAPS-1D software. ZnO is used as common electron transfer medium (ETM), whereas Cu_2O , CuI and CuO materials are separately used for hole transfer medium (HTM) each time. The cell basic parameters (V_{oc} , J_{sc} , FF and efficiency) are simulated at various conditions. CuO is found to be the best HTM material, whereas the maximum efficiency of 26.8 % is obtained at 0.55 μm thickness of $\text{CH}_3\text{NH}_3\text{PbI}_{3-x}\text{Cl}_x$ material with a donor atom density of about 10^{17} cm^{-3} .

Keywords: *Perovskite Solar Cells, Optimization, SCAPS*

$\text{CH}_3\text{NH}_3\text{PbI}_{3-x}\text{Cl}_x$ Bazlı Perovskite Güneş Hücrelerinin Sayısal Analizi ve Optimizasyonu

ÖZET

Perovskite malzemelerinin benzersiz özelliklerinden dolayı, söz konusu malzemelerden üretilen güneş pili teknolojilerinin verimliliği, maksimum teorik noktası olan %32'ye doğru hızla ilerlerlemektedir. Bu çalışmada, SCAPS-1D yazılımını kullanılarak $\text{CH}_3\text{NH}_3\text{PbI}_{3-x}\text{Cl}_x$ bazlı perovskite güneş pilli tasarlanıp, parametreleri simüle edildi. ZnO, ortak elektron transfer katmanı (ETM) olarak kullanılırken, hol transfer katmanı (HTM) için Cu_2O , CuI ve CuO malzemeleri her seferinde ayrı ayrı kullanıldı. Hücre temel parametreleri (V_{oc} , J_{sc} , FF ve verimlilik) farklı koşullarda simüle edildi. CuO en iyi HTM malzemesi olarak gözlemlenirken, yaklaşık 10^{17} cm^{-3} verici atom yoğunluğunda ve 0.55 μm kalınlığındaki $\text{CH}_3\text{NH}_3\text{PbI}_{3-x}\text{Cl}_x$ materyalinde maksimum %26.8 verimlilik elde edildi.

Anahtar Kelimeler: *Perovskite Güneş Pilleri, Optimizasyon, SCAPS*

I. INTRODUCTION

Perovskite solar cells have shown rapid progress in last decade due to their unique properties. They are considered to overcome the current PV conversion limit as perovskite solar cells exhibit high absorption coefficient, long carrier diffusion length and lifetime and high carrier mobility [1][2][3]. As well as having suitable band gap for exploiting much of solar energy, perovskite solar cells have cost effective and easy fabrication techniques and are compatible with flexible substrates. The efficiency for those PV technology has increased from ~3% in 2009[4] to ~25 % in 2020[5].

Hitherto variety of perovskite materials, cell structures, hole transfer mediums (HTM), electron transfer mediums (ETM) and electrodes have been used to optimize the cell efficiency. Initially liquid electrolyte was used as HTM which inhibited the performance of the cell in minutes due to ionic nature of the Perovskite materials[4]. However after development of solid state functional HTM materials, the efficiency and stability of those solar cells have improved tremendously[6]. $\text{CH}_3\text{NH}_3\text{PbI}_{3-x}\text{Cl}_x$ perovskite material is one most studied absorbers due its excellent optical band gap and absorption cross section [3]. Currently the main challenges for those technology are that long term stability, charge recombination losses that take place at the perovskite material and interfaces between perovskite/HTM and perovskite/ETM[7]. To obtain deep knowledge of those losses more experimental and theoretical research need to be carried out.

In this study, we modelled a perovskite solar cell device with a construction of ETM/ $\text{CH}_3\text{NH}_3\text{PbI}_{3-x}\text{Cl}_x$ /HTM using Solar Cell Capacitance Simulator (SCAPS) software. As ETM material ZnO at different thicknesses was used while as HTM Cu_2O , CuI and CuO materials at different thicknesses, donor concentration levels and temperatures were tried one by one. The reason we preferred Cu_2O , CuI and CuO materials as HTM layer is that these materials are cost effective and have high stability against ambient conditions[8]. It is found that the best efficiency was obtained when using CuO as HTM material.

II. DEVICE SIMULATION

SCAPS software simulates thin film solar cells in one dimension using drift-diffusion equations for holes and electrons and Poisson's equations[9]. The software also includes the thermionic emissions from device surfaces.

The architecture and the energy band diagram of the proposed planar structure perovskite solar cell are shown in Figure 1a&b, respectively. Fluorine doped tin oxide coated glass (FTO) and gold (Au) are used as front and back contacts, respectively. ZnO and $\text{CH}_3\text{NH}_3\text{PbI}_{3-x}\text{Cl}_x$ are used as ETM and absorber, respectively, while for HTM Cu_2O , CuI and CuO materials are alternated. Each design construction is carefully selected and the parameters for each layer are obtained from literature and tabulated in Table 1. The extra parameters of back and front contacts are given in Table 2. Unless otherwise is stated the parameters are used as in the Table 1&2. All results are obtained under AM1.5G 100 mW/cm^2 illumination conditions.

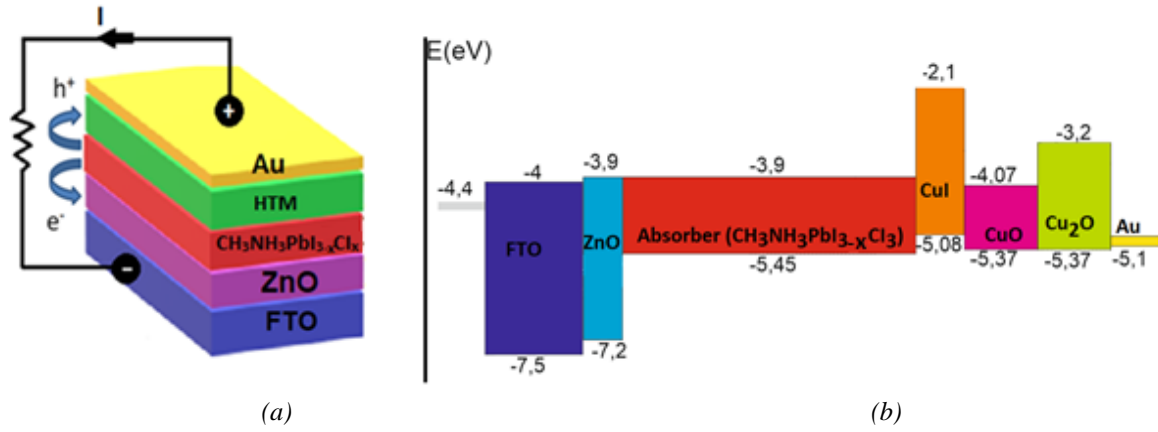


Figure 1. The geometry structure (a) and the schematic band diagram (b) of the simulated solar cell. For each device design only one HTM material is used.

Table 1. Input physical parameters of the materials used to build the perovskite cell. [10][11][12][13][14][15][16][17]

Parameters	FTO	ZnO	CH ₃ NH ₃ PbI _{3-x} Cl _x	CuI	CuO	Cu ₂ O
Thickness (nm)	200	80	600	100	150	150
Bandgap energy, E _g (eV)	3.5	3.3	1.55	2.98	1.3	2.17
Electron affinity, (eV)	4	3.9	3.9	2.1	4.07	3.2
Relative dielectric permittivity, ε _r	9	9	6.5	6.5	18.1	7.11
CB effective density of states, (1/cm ³)	2.2×10 ¹⁸	10 ¹⁹	2.2×10 ¹⁸	2.8×10 ¹⁹	2.2×10 ¹⁸	2.2×10 ¹⁸
VB effective density of states (1/cm ³)	1.8×10 ¹⁹	1×10 ¹⁹	1.8×10 ¹⁹	10 ¹⁹	1.8×10 ¹⁹	1.8×10 ¹⁹
Electron thermal velocity (cm/s)	10 ⁷	10 ⁷	10 ⁷	10 ⁷	10 ⁷	10 ⁷
Hole thermal velocity (cm/s)	10 ⁷	10 ⁷	10 ⁷	10 ⁷	10 ⁷	10 ⁷
Mobility of electron(cm ² /Vs)	20	50	2	1.69×10 ⁻⁴	0.1	80
Mobility of hole(cm ² /Vs)	10	5	2	1.69×10 ⁻⁴	0.1	80
Donor density (1/cm ³), (N _D)	10 ¹⁸	5×10 ¹⁷	10 ¹³	0	0	0
Acceptor density (1/cm ³), (N _A)	0	0	0	10 ¹⁸	10 ¹⁸	10 ¹⁸
Defect density (1/cm ³) (N _T)	10 ¹⁵	10 ¹⁵	2.5×10 ¹³	10 ¹⁵	10 ¹⁵	10 ¹⁵

Table 2. The basic material parameters of the back and front contacts.

Electrical properties@ 300 K	Back contact (Au)	Front contact (FTO)
Thermionic emission/surface recombination velocity of electron(cm/s)	10 ⁵	10 ⁷
Thermionic emission/surface recombination velocity of hole(cm/s)	10 ⁷	10 ⁵
Work function(eV)	5.1	4.4

III. RESULTS AND DISCUSSIONS

Since the absorber parameters and its physical size and geometry are significant factors for device efficiency, we initially investigate the impact of perovskite absorber thickness on the device electrical parameters. All other layer parameters are set to be same, HTM was chosen CuO and $\text{CH}_3\text{NH}_3\text{PbI}_{3-x}\text{Cl}_x$ thickness are varied from 0.1 μm to 1 μm and the device performance was recorded. The same process was repeated using CuI and Cu_2O as HTM material. The cell efficiency variations as a function of absorber thickness for three different HTM materials are shown in Figure 2.

For all HTM materials, the thickness increases from 0.1 μm to about 0.55 μm , the efficiency increases after that point it decreases with increasing the thicknesses. CuO exhibits best results compared with the other two HTM materials. All other cell parameters obtained for three HTM materials are compiled in Table 3.

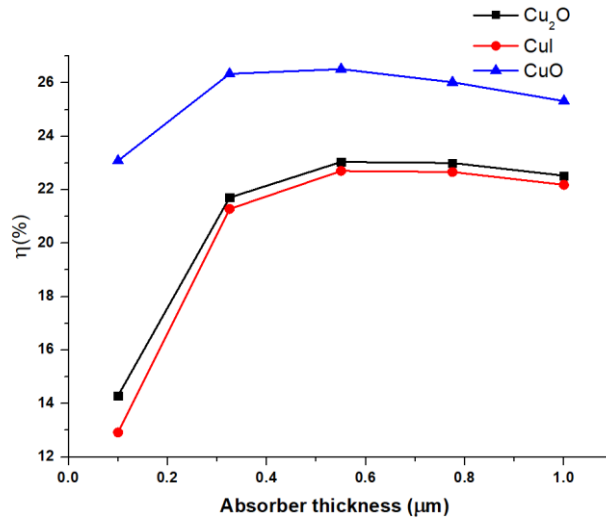


Figure 2. The relationship between the cell efficiency and the absorber thickness.

Table 3. The variation of cell parameters (V_{OC} , J_{SC} , FF) with the five different absorber thickness at 10^{13} absorber N_D value.

HTM material	Absorber Thickness (μm)	V_{OC} (V)	J_{SC} (mA/cm^2)	FF (%)
CuI	0.1	1.18	13.03	83.84
	0.325	1.13	22.43	83.71
	0.55	1.1	24.76	82.67
	0.775	1.09	25.54	81.24
	1	1.07	25.84	79.51
CuO	0.1	1.45	22.63	70.35
	0.325	1.176	27.1	82.56
	0.55	1.123	28.29	83.38
	0.775	1.1	28.69	82.22
	1	1.08	28.84	80.57
Cu_2O	0.1	1.34	14.24	74.91
	0.325	1.15	22.55	83.24
	0.55	1.11	24.78	83.43
	0.775	1.1	25.54	82.1
	1	1.08	25.85	80.44

The cell short-circuit current density (J_{sc}) increases with the increasing the absorber thickness for all HTM materials. However, at thicker absorber values the open circuit voltage (V_{oc}) decreases for each HTM material. Hence fill factor (FF) and efficiency show maximum values at about 0.6 μm . the best performing HTM material is CuO wherein all cell parameters are recorded to be higher than that of two other materials.

Since diffusion length of $\text{CH}_3\text{NH}_3\text{PbI}_{3-x}\text{Cl}_x$ perovskite films is about 450 nm [18], until that point the device efficiency increases and after that point the efficiency decreases with absorber thickness due to increase of the charge carrier recombination loss. As the absorber thickness increases, more electron hole pairs contribute to the photocurrent[18] and hence J_{sc} increases with increasing the absorber thickness. V_{oc} strongly depend on the charge recombination related losses and hence as the absorber thickness increases V_{oc} falls[19]. FF is related to the power loss on the device interior load and hence as the absorber thickness increases, the FF value declines. Overall the results agree with the previous reports carried out for different materials [10][20].

To observe the effect of the donor atom density (N_D) in the perovskite absorber on the cell parameters, we spanned N_D values from 10^9 cm^{-3} to 10^{17} cm^{-3} at 0.6 μm absorber thickness, as shown in Figure 3 and Table 4.

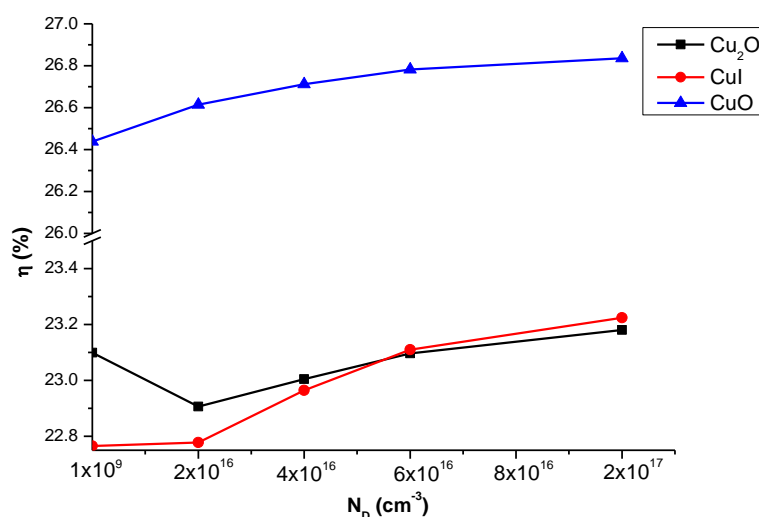


Figure 3. The variation of efficiency with the donor atom density of perovskite layer for three HTM materials.

Table 4. The cell parameters at different absorber doping levels for CuI, CuO and Cu₂O HTM materials.

HTM material	Absorber N_D (cm^{-3})	V_{oc} (V)	J_{sc} (mA/cm^2)	FF (%)
CuI	1×10^9	1.1	25	82.4
	2.5×10^{16}	1.16	23.5	83.3
	5×10^{16}	1.18	23	84.57
	7.5×10^{16}	1.19	22.76	85.27
	1×10^{17}	1.19	22.61	85.75
CuO	1×10^9	1.117	28.42	83.23
	2.5×10^{16}	1.27	27.11	74.24
	5×10^{16}	1.38	26.62	72.28
	7.5×10^{16}	1.47	26.38	68.71
	1×10^{17}	1.54	26.23	66.05
Cu ₂ O	1×10^9	1.11	25.02	83.2
	2.5×10^{16}	1.27	23.54	76.63
	5×10^{16}	1.42	23.02	70.15
	7.5×10^{16}	1.57	22.76	64.67
	1×10^{17}	1.71	22.6	59.98

Overall both efficiency and other cell parameters initially increase with doping density until about $6 \times 10^{16} \text{ cm}^{-3}$ then their rising rate slow considerably. The maximum cell efficiency (26.8 %) is recorded at 10^{17} cm^{-3} doping level for CuO HTM material. The reason why increase in perovskite N_D value raises the cell efficiency is that in the indicated N_D region, each additional donor atom will increase the number of the free electrons and consequently the photocurrent will increase [21].

The ETM material parameters are crucial for the device efficiency. To observe what extent it is important for the cell, we simulated the device at different ZnO thickness for three different HTM materials. All obtained solar cell parameters are summarised in Table 5 and the efficiency variations with shell thickness for three different HTM materials are compared in Figure 4. As seen from the Table 5, as ZnO thickness increases V_{oc} and FF values do not change in the case of three HTM layers, while J_{sc} slightly decreases with increasing ZnO thicknesses for three HTM materials. The increase in ZnO thickness to some extent raises the cell efficiency as seen in Figure 4. As in previous cases, CuO HTM material again showed maximum J_{sc} (28.4 mA/cm²), FF (83.23%), and η (26.4%) values compared with CuI and Cu₂O materials. Since the ETM layer is in the front contact of the device, a portion of the incident light attenuates in this layer and hence at the thicker ETM levels the efficiency decreases gradually.

Table 5. The relationship between ZnO thickness and cell parameters (V_{oc} , J_{sc} , FF).

HTM materials	ZnO Thickness (μm)	V_{oc} (V)	J_{sc} (mA/cm ²)	FF (%)
CuI	0.01	1.11	25.05	82.39
	0.26	1.1	25.25	82.39
	0.51	1.1	24.97	82.39
	0.76	1.1	24.91	82.39
	1	1.1	24.85	82.39
CuO	0.01	1.11	28.42	83.22
	0.26	1.11	28.44	83.23
	0.51	1.11	28.38	83.23
	0.76	1.11	28.33	83.23
	1	1.11	28.26	83.23
Cu ₂ O	0.01	1.11	25.02	83.18
	0.26	1.11	25.01	83.19
	0.51	1.11	24.98	83.19
	0.76	1.11	24.92	83.19
	1	1.11	24.86	83.19

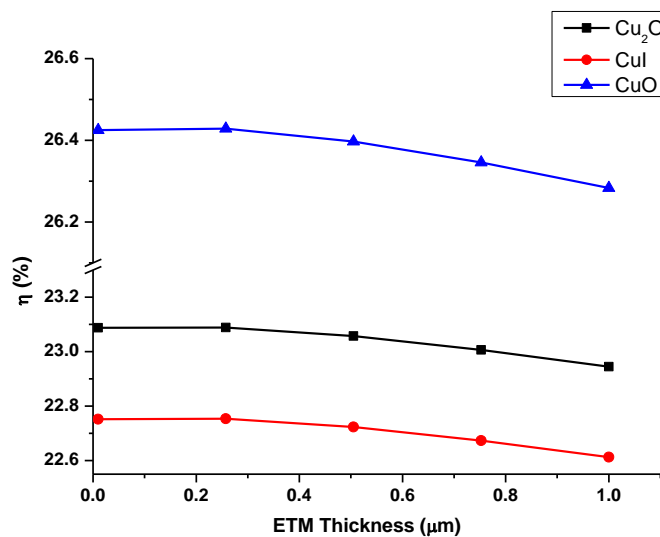


Figure 4. The variation of cell efficiency as a function of ZnO layer thickness.

To understand the effect of ZnO layer further on the solar cell parameters, we obtained cell parameter at different donor atom concentrations (N_D) of ZnO layer, as seen in Table 6 and Figure 5. As N_D values for ZnO material span from 10^{13} cm^{-3} to 10^{22} cm^{-3} V_{oc} and J_{sc} remain almost constant for all HTM materials. FF and η values for all HTM materials increased while moving from 10^{13} cm^{-3} to 10^{22} cm^{-3} then remained constant.

An appropriate donor concentration value helps to increase the cell efficiency. However at very high donor atom concentration levels the ZnO material becomes degenerated and fermi energy level lies within the conduction band [20]. Therefore, the device parameters are saturated which is the case we see here.

Table 6. V_{oc} , J_{sc} , and FF values obtained for three different hole transfer materials at different ZnO N_D concentrations. (ZnO thickness is set be $0.080 \mu\text{m}$)

HTM materials	ZnO N_D (cm^{-3})	V_{oc} (V)	J_{sc} (mA/cm^2)	FF (%)
CuI	5×10^{13}	1.09	25.01	81.75
	1.25×10^{22}	1.1	24.92	82.46
	2.5×10^{22}	1.1	24.92	82.46
	3.75×10^{22}	1.1	24.92	82.46
	5×10^{22}	1.1	24.92	82.46
CuO	5×10^{13}	1.11	28.42	82.56
	1.25×10^{22}	1.11	28.34	83.4
	2.5×10^{22}	1.11	28.34	83.4
	3.75×10^{22}	1.11	28.34	83.4
	5×10^{22}	1.11	28.34	83.4
Cu ₂ O	5×10^{13}	1.1	25.02	82.53
	1.25×10^{22}	1.11	24.93	83.26
	2.5×10^{22}	1.11	24.93	83.26
	3.75×10^{22}	1.11	24.93	83.26
	5×10^{22}	1.11	24.93	83.26

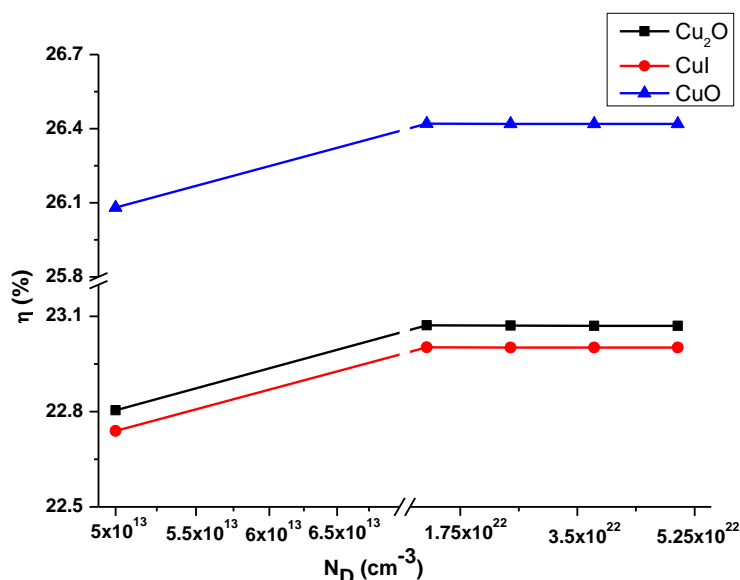


Figure 5. The relationship between ZnO layer donor atom concentration and device efficiency.

HTM material and its size and geometry play important role in the efficiency of solar cell devices. Hence to understand what degree it affect the cell parameters, we calculated V_{oc} , J_{sc} , FF and η values at different HTM thicknesses, spanning from 0.1 μm to 1 μm , for three HTM layers. The results are shown in Table 7 and Figure 6. Overall, V_{oc} does not change with thickness for all materials. While J_{sc} for CuI does not change with changing the thickness, it slightly increases with increasing the HTM layer thickness for CuO and Cu_2O materials. In the cases of CuI and CuO layers, FF value decreases with increasing layer thickness, whereas it remains constant in the case of Cu_2O HTM material.

As seen in the figure the efficiency initially increases from 22.5% to 23.2% then stay flat for the rest of thicknesses for CuO material, whereas it remains constant for all thicknesses for Cu_2O material. However, the efficiency considerably decreases with increasing the CuI HTM layer thickness. The main reason for the best cell performance occur at thin HTM levels is that the time for holes to reach the counter electrode decreases[20]. More research is needed to explain the effect of HTL thickness on the cell parameters in details.

Table 7. V_{oc} , J_{sc} , and FF values obtained at 10 different thicknesses of each hole transfer materials (N_A for HTM materials are set to be 10^{18} cm^{-3}).

HTM material	HTM Thickness (μm)	V_{oc} (V)	J_{sc} (mA/cm^2)	FF (%)
CuI	0.100	1.11	25	74.13
	0.200	1.11	25	73.45
	0.300	1.11	25	72.77
	0.400	1.11	24.99	72.09
	0.500	1.11	24.99	71.42
	0.600	1.11	24.99	70.74
	0.700	1.11	24.99	70.07
	0.800	1.11	24.99	69.4
	0.900	1.11	24.99	68.74
	1.000	1.11	24.99	68.07
CuO	0.100	1.05	25.276	84.64
	0.200	1.058	25.809	83.96
	0.300	1.056	26.129	83.59
	0.400	1.059	26.28	83.42
	0.500	1.059	26.344	83.34
	0.600	1.06	26.37	83.31
	0.700	1.06	26.381	83.29
	0.800	1.06	26.385	83.29
	0.900	1.06	26.384	83.28
	1	1.06	26.388	83.28
Cu_2O	0.100	1.109	25.177	83.19
	0.200	1.109	25.0224	83.19
	0.300	1.109	25.025	83.19
	0.400	1.109	25.028	83.19
	0.500	1.109	25.03	83.19
	0.600	1.109	25.032	83.19
	0.700	1.109	25.034	83.19
	0.800	1.109	25.035	83.19
	0.900	1.109	25.036	83.19
	1	1.109	25.037	83.19

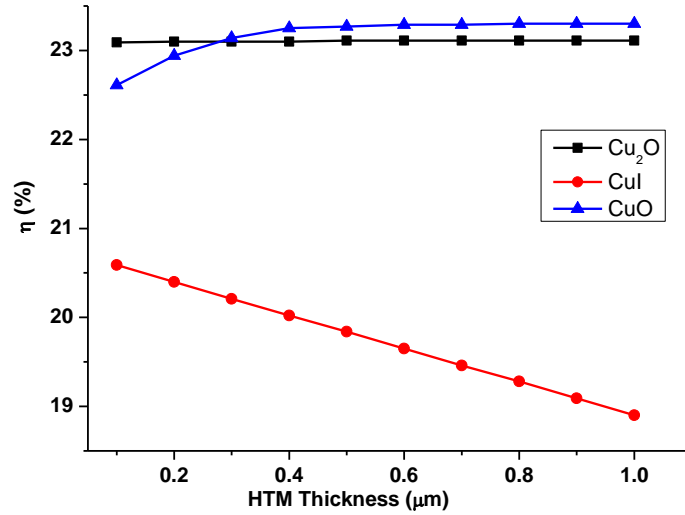


Figure 6. The variation of cell efficiency as a function of HTM layer thickness for three materials.

Since ambient temperature is another key parameter regarding device efficiency, we simulated the cell parameters at different working temperatures and the results are summarized in Table 8 and Figure 7. As temperature increases V_{oc} values for all materials decrease whereas, J_{sc} values for Cu_2O and CuI nearly remain constant and for CuO it slightly increases. Although FF values for CuO and Cu_2O HTM layers decrease considerably with increasing the temperature, it increases steadily in the case of CuI layer. Finally, the device efficiencies significantly decrease with rising the temperature for all materials.

Ideally as the temperature increases the bandgap of the absorber decreases which result in more electron-hole pair generation [22]. However, the diffusion length and charge carrier mobility in perovskite films decrease with increasing the temperature[20]. The latter effect suppresses the former effect and hence the overall efficiency decreases with increasing the temperature.

Table 8. V_{oc} , J_{sc} , and FF values obtained for three different hole transfer materials at 5 different temperature values. (N_A for Cu_2O , CuO , and CuI is set to 10^{18} cm^{-3} , layer thickness for CuI , CuO and Cu_2O materials are kept to be $0.1 \mu\text{m}$, $0.15 \mu\text{m}$ and $0.15 \mu\text{m}$, respectively.)

HTM material	Temperature (K)	V_{oc} (V)	J_{sc} (mA/cm^2)	FF (%)
CuI	273	1.15	25	72.51
	295	1.12	25	73.87
	312	1.1	24.99	74.82
	339	1.1	24.99	75.33
	360	1.1	24.99	75.31
CuO	273	1.1	25.33	84.98
	295	1.06	25.51	84.5
	312	1.02	25.71	83.59
	339	0.989	25.927	82.56
	360	0.95	26.123	81.49
Cu₂O	273	1.196	25.021	83.94
	295	1.121	25.02	83.4
	312	1.08	25.019	82.45
	339	1.04	25.018	81.34
	360	1.001	25.017	80.14

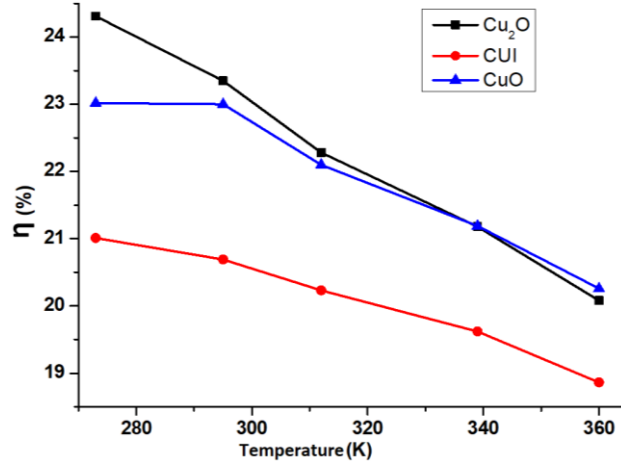


Figure 7. The variation the device efficiency as a function of operational temperature for three HTM materials.

Since CuO is found to be the most efficient HTM material, we added J-V characteristics of the proposed perovskite solar cells using CuO as the HTM material, as shown in Figure 8. The cell parameters are chosen to be as in the Table 1 and 2. As seen from the figure that J_{sc} value is about 25.5 mA/cm^2 , while V_{oc} value is about 1.07 V . The obtained cell parameter values are consistent with the results reported in the literature for $\text{CH}_3\text{NH}_3\text{PbI}_{3-x}\text{Cl}_x$ based perovskite solar cells using different HTM material [23].

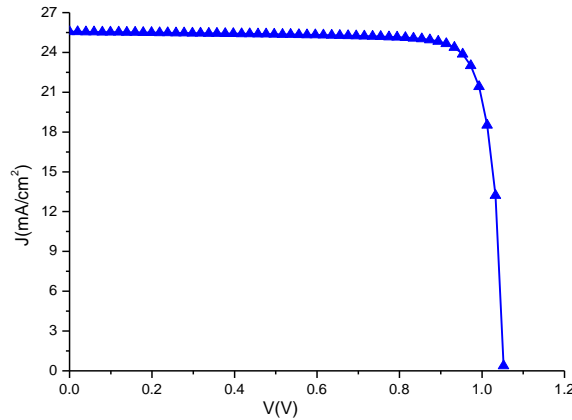


Figure 8. J-V characteristics of the proposed perovskite solar cell using CuO as the HTM material.

IV. CONCLUSION

$\text{CH}_3\text{NH}_3\text{PbI}_{3-x}\text{Cl}_x$ based perovskite solar cell is designed and simulated using SCAPS-1D software. All results are compared for three different HTM materials (CuO, CuI, Cu_2O) and CuO is found to be the best candidate. The maximum efficiency of of $\sim 26.8 \%$ is recorded at the absorber thickness of around $0.55 \mu\text{m}$ and at the absorber donor atom density of about 10^{17} cm^{-3} . The cell parameters are found to be significantly affected by thickness and donor atom density of the ETM layer. HTM layer thickness and cell operating temperature also affect the cell parameters. The obtained results are consistent with the results reported in the literature. This work will contribute to the progress of the perovskite solar cells; in particularly will have important implications in the optimizations of absorber thickness and doping concentration and charge transport layers and operating temperatures.

ACKNOWLEDGEMENTS: The authors are thankful to Prof. Marc Burgelman at the University of Gent for providing SCAPS-1D software.

V. REFERENCES

- [1] N. G. Park, “Perovskite solar cells: An emerging photovoltaic technology,” *Materials Today*, vol. 18, no. 2, pp. 65–72, 01-Mar-2015.
- [2] S. D. Stranks *et al.*, “Electron-hole diffusion lengths exceeding 1 micrometer in an organometal trihalide perovskite absorber,” *Science*, vol. 342, no. 6156, pp. 341–344, Oct. 2013.
- [3] M. A. Green, A. Ho-Baillie, and H. J. Snaith, “The emergence of perovskite solar cells,” *Nat. Photonics*, vol. 8, no. 7, pp. 506–514, 2014.
- [4] A. Kojima, K. Teshima, Y. Shirai, and T. Miyasaka, “Organometal halide perovskites as visible-light sensitizers for photovoltaic cells,” *J. Am. Chem. Soc.*, vol. 131, no. 17, pp. 6050–6051, 2009.
- [5] M. Jeong *et al.*, “Stable perovskite solar cells with efficiency exceeding 24.8% and 0.3-V voltage loss,” *Science*, vol. 369, no. 6511, pp. 1615–1620, 2020.
- [6] H. S. Kim *et al.*, “Lead iodide perovskite sensitized all-solid-state submicron thin film mesoscopic solar cell with efficiency exceeding 9%,” *Sci. Rep.*, vol. 2, no. 1, pp. 1–7, 2012.
- [7] J. P. Correa-Baena *et al.*, “Promises and challenges of perovskite solar cells,” *Science*, vol. 358, no. 6364, 2017.
- [8] C. Zuo and L. Ding, “Solution-Processed Cu₂O and CuO as Hole Transport Materials for Efficient Perovskite Solar Cells,” *Small*, vol. 11, no. 41, pp. 5528–5532, 2015.
- [9] M. Burgelman, P. Nollet, and S. Degraeve, “Modelling polycrystalline semiconductor solar cells,” *Thin Solid Films*, vol. 361, pp. 527–532, 2000.
- [10] K. Tan, P. Lin, G. Wang, Y. Liu, Z. Xu, and Y. Lin, “Controllable design of solid-state perovskite solar cells by SCAPS device simulation,” *Solid. State. Electron.*, vol. 126, pp. 75–80, 2016.
- [11] G. A. Casas, M. A. Cappelletti, A. P. Cédola, B. M. Soucase, and E. L. Peltzer y Blancá, “Analysis of the power conversion efficiency of perovskite solar cells with different materials as Hole-Transport Layer by numerical simulations,” *Superlattices Microstruct.*, vol. 107, pp. 136–143, 2017.
- [12] L. Zhu, G. Shao, and J. K. Luo, “Numerical study of metal oxide heterojunction solar cells,” *Semicond. Sci. Technol.*, vol. 26, no. 8, 2011.
- [13] M. Goudarzi and M. Banihashemi, “Simulation of an inverted perovskite solar cell with inorganic electron and hole transfer layers (Erratum),” *J. Photonics Energy*, vol. 7, no. 2, pp. 029901, 2017.
- [14] T. Minemoto and M. Murata, “Impact of work function of back contact of perovskite solar cells without hole transport material analyzed by device simulation,” *Curr. Appl. Phys.*, vol. 14, no. 11, pp. 1428–1433, 2014.
- [15] S. J. Fonash, “Material Properties and Device Physics Basic to Photovoltaics,” in *Solar Cell Device Physics*, Elsevier, 2010, pp. 9–65.
- [16] Z. El Jouad, M. Morsli, G. Louarn, L. Cattin, M. Addou, and J. C. Bernède, “Improving the efficiency of subphthalocyanine based planar organic solar cells through the use of MoO₃/CuI double anode buffer layer,” *Sol. Energy Mater. Sol. Cells*, vol. 141, pp. 429–435, 2015.

- [17] F. Liu *et al.*, “Numerical simulation: Toward the design of high-efficiency planar perovskite solar cells,” *Appl. Phys. Lett.*, vol. 104, no. 25, 2014.
- [18] T. M. Koh *et al.*, “Formamidinium tin-based perovskite with low E_g for photovoltaic applications,” *J. Mater. Chem. A*, vol. 3, no. 29, pp. 14996–15000, 2015.
- [19] C. M. Wolff, P. Caprioglio, M. Stolterfoht, and D. Neher, “Nonradiative Recombination in Perovskite Solar Cells: The Role of Interfaces,” *Adv. Mater.*, vol. 31, no. 52, 2019.
- [20] M. Kumar, A. Raj, A. Kumar, and A. Anshul, “An optimized lead-free formamidinium Sn-based perovskite solar cell design for high power conversion efficiency by SCAPS simulation,” *Opt. Mater. (Amst.)*, vol. 108, pp. 110213, 2020.
- [21] S. O. Kasap, *Optoelectronics & Photonics: Principles & Practices: International Edition*, 2nd ed. Pearson Education Limited, 2013, ch. 5, pp. 437
- [22] D. A. Neamen, *Semiconductor Physics And Devices: Basic Principles*, 4th ed. McGraw-Hill, 2012.
- [23] W. Isoe, M. Mageto, C. Maghanga, M. Mwamburi, V. Odari, and C. Awino, “Thickness Dependence of Window Layer on CH₃NH₃PbI₃-XClX Perovskite Solar Cell,” *Int. J. Photoenergy*, vol. 2020, 2020.